

A SURVEY FOR FAST TRANSIENTS IN THE FORNAX CLUSTER OF GALAXIES

A. RAU,¹ E. O. OFEK,¹ S. R. KULKARNI,¹ B. F. MADORE,² O. PEVUNOVA,³ AND M. AJELLO⁴

Received 2008 January 8; accepted 2008 April 25

ABSTRACT

The luminosity gap between novae ($M_R \leq -10$) and supernovae ($M_R \geq -14$) has been well known since the pioneering research of Zwicky and Hubble. Nearby galaxy clusters and concentrations offer an excellent opportunity to search for explosions brighter than classical novae and fainter than supernovae. Here we present the results of a B -band survey of 23 member galaxies of the Fornax Cluster, performed at the Las Campanas 2.5 m Irénée du Pont telescope. Observations with a cadence of 32 minutes discovered no genuine fast transient to a limiting absolute magnitude of $M_B = -9.3$ mag. We provide a detailed assessment of the transient detection efficiency and the resulting upper limits on the event rate as function of peak magnitude. Further, we discuss the discoveries of five previously unknown foreground variables which we identified as two flare stars, two W UMa-type eclipsing binaries and a candidate δ Scuti/SX Phe star.

Subject headings: δ Scuti — stars: flare — stars: variables: other — surveys

Online material: machine-readable table

1. INTRODUCTION

The recent findings of a number of enigmatic transients, e.g., new types of novae- (Kulkarni et al. 2007) and supernovae-related events (Ofeek et al. 2007; Smith et al. 2007; Quimby et al. 2007; Pastorello et al. 2007), have demonstrated that the phase space of eruptive transients is already richer than discussed in astronomy texts. Even more discoveries, especially on timescales of days to weeks, are anticipated for the upcoming large-area facilities, such as SkyMapper (Schmidt et al. 2005), the Panoramic Survey Telescope and Rapid Response System (Pan-STARRS; Kaiser et al. 2002), and the Large Synoptic Survey Telescope (LSST; Tyson 2005). However, on shorter timescales (minutes to hours), their observational designs are less optimal and dedicated, small experiments are more likely to lead to great findings. A small number of such surveys have been performed previously (e.g., Becker et al. 2004; Rykoff et al. 2005; Morales-Rueda et al. 2006; Ramsay et al. 2006) and informed us of the difficulty of discovering genuine new classes of fast transients and variables.⁵ Here the greatest challenge is to pierce the fog of known foreground contaminants. Asteroids and flares from M dwarfs have been established to dominate the short-timescale variable sky (Kulkarni & Rau 2006). However, once this curtain is penetrated, exciting and rare events can be found, e.g., the high-amplitude optical flickering (~ 3.5 mag in 6 minutes) accompanying the outburst of the Galactic X-ray binary Swift J195509.6+261406 (Stefanescu et al. 2007; Kasliwal et al. 2008). The latter source was brought to attention by its preceding gamma-ray flare (Pagani et al. 2007). Nonetheless, high-cadence optical surveys will be capable of detecting similar events independently of the high-energy emission.

Another, yet unidentified, bright ($R = 11.7$ mag), high-amplitude candidate transient (>6 mag in 2 minutes) was recently discovered along the line of sight to the nearby (~ 70 Mpc) galaxy IC 4779 (Klotz et al. 2007). If associated with IC 4779, the event reached a staggering peak luminosity of $L_{R,\text{peak}} \sim 3 \times 10^{44}$ ergs s⁻¹, outshined only by the brightest known supernova (SN 2005ap; Quimby et al. 2007).

A critical component of every successful transient search is a judicious target selection. This is especially relevant for short-cadence experiments, in which only a small number of fields are repeatedly observed. Obvious targets for such a search are nearby massive clusters of galaxies. Clusters contain a large stellar mass, which increases the probability of finding rare events during the transient phase. Furthermore, their known distance provides a direct access to the absolute brightness of the events. In addition, the variety of galaxy types, and thus stellar populations, may offer constraints on the progenitor ages.

In this paper we present the results of an optical survey of galaxies in the Fornax Cluster designed to test the transient and variable sky in a galaxy cluster environment on timescales shorter than 1 hr. At the distance of 16.2 ± 1.5 Mpc [$(m - M)_0 = 30.91 \pm 0.19$; Grillmair et al. 1999] and with negligible foreground extinction [$E(B - V) = 0.013$ mag; Schlegel et al. 1998] observations of the Fornax Cluster allow one to probe the gap in absolute peak brightness between classical novae ($M_R > -10$) and supernovae ($M_R < -14$) with even 2 m class telescopes. This part of phase space has become particularly alluring with the recognition of an emerging population of new types of explosions, namely, the luminous red novae (Kulkarni et al. 2007; Rau et al. 2007; Ofek et al. 2008).

2. OBSERVATIONS AND DATA REDUCTION

Observations were obtained with the Wide Field Reimaging CCD Camera (WFCCD) at the 2.5 m Irénée du Pont telescope in Las Campanas, Chile. The detector dimensions of 2048×2048 pixels, together with the plate scale of $0.774''$, provide a circular field of view with $\sim 12.5'$ radius. Imaging was performed in the B band as a compromise between avoiding flares from Galactic M dwarfs (especially bright in the ultraviolet) and increasing the contrast between possible transients and the

¹ Caltech Optical Observatories, Mail Stop 105-24, California Institute of Technology, Pasadena, CA 91125.

² Observatories of the Carnegie Institution of Washington, 813 Santa Barbara Street, Pasadena, CA 91101.

³ Infrared Processing and Analysis Center, Mail Stop 100-22, Jet Propulsion Laboratory, California Institute of Technology, Pasadena, CA 91125.

⁴ Max-Planck-Institut für extraterrestrische Physik, Giessenbachstrasse 1, 80748 Garching, Germany.

⁵ In the following we refer to an event as transient when it has no known quiescent counterpart at any wavelength and to a source which shows a quiescent counterpart in our images or has a cataloged counterpart as variable.

TABLE 1
FIELDS

Field	R.A. _{J2000.0} ^a	Decl. _{J2000.0} ^a	Galaxies ^b
A.....	03 24 36.7	−36 26 21	NGC 1326, 1326A, 1326B
B.....	03 22 41.1	−37 10 54	NGC 1316, 1317
C.....	03 31 04.3	−33 36 42	NGC 1350
D.....	03 36 29.5	−34 52 28	NGC 1380, 1380A
E.....	03 35 44.1	−35 18 50	NGC 1373, 1374, 1375, 1379, 1381
F.....	03 36 49.0	−35 20 55	NGC 1379, 1381, 1382, 1387, MCG 06-09-008
G.....	03 38 34.0	−35 29 58	NGC 1399, 1404
H.....	03 36 45.2	−36 06 17	NGC 1369, 1386
I.....	03 33 37.5	−36 07 19	NGC 1365
K.....	03 42 21.9	−35 16 12	NGC 1427, 1428

NOTE.—Units of right ascension are hours, minutes, and seconds, and units of declination are degrees, arcminutes, and arcseconds.

^a Coordinates of the centers of the fields.

^b Prominent galaxies within the field of view.

predominantly early-type cluster galaxies (bright in the red part of the spectrum).

For the survey, we selected 10 fields covering the 23 brightest Fornax I Cluster members (Table 1, Fig. 1). These fields were imaged with a sequence of 120 s exposures repeated up to 15 times in each of five nights in 2006 October and December. Additional single exposures were obtained in five nights in 2006 November (see Table 2 for a complete log). As part of a sequence, a single exposure was taken at each position, after which the telescope slewed to the next field. The resulting distribution of times between consecutive images for each field is given in Figure 2. Throughout the survey a mean intraday cadence of $\Delta t = 32.25$ minutes was achieved. The spread of the observations between 2006 October and December allowed for the possible detection of slowly evolving events with timescales of about 1 month (e.g., supernovae).

Figure 2 indicates that our primary sensitivity is to variability on ~ 32 minute timescales. Here we have a total exposure time of 13.7 days distributed over 616 images (neglecting the once-per-day exposures in November). With a covered area of 0.136 deg^2 per image, this yields a total areal exposure, E_A , of $1.86 \text{ deg}^2 \text{ days}$. We have a factor of 5 and 44 larger E_A for internight and inter-month observation intervals, respectively.

Image reduction (bias subtraction, flat fielding) was performed using standard IRAF routines.⁶ The astrometric solutions were obtained in reference to NOMAD⁷ with ASCfit, version 3.0.⁸ The strategy to search for transients and variables in single exposures implies that cosmic-ray removal by median combining of multiple images was not applicable. Hence, we applied a Laplacian algorithm (lacos_im; van Dokkum 2001) which allows the identification of cosmic rays in single frames.

For absolute photometric calibration we used observations of the standard star field T Phe (Landolt 1992) taken under photometric conditions (2006 November 19). This calibration was applied to the images of the 10 Fornax fields obtained during the same night. Exposures from the remaining nights were tied relatively to these absolutely calibrated frames. Here we selected an ensemble of at least 40 local, nonsaturated, nonvariable ($\Delta B < 0.01 \text{ mag}$) reference stars for each image. The photo-

metric offset between the two observations was estimated by deriving the median brightness offset of these sets of stars with respect to their brightness in the reference frame. This was successively done for all observations of a given field, thus providing a common photometric zero point. The resulting photometric accuracy for point sources is shown in Figure 3. In a typical night a 5σ limiting magnitude of $B \sim 22 \text{ mag}$ was reached. Sources brighter than $B \sim 15 \text{ mag}$ were generally saturated.

The search for transients and variables was performed in two separate steps. First we applied a point-spread function (PSF)-matched image subtraction using a software package based on ISIS (Alard 2000). Reference frames for all fields were generated by combining the three best quality exposures taken in 2006 November. Candidate transients and variables were detected in the difference images using SExtractor, version 2.5.0 (Bertin & Arnouts 1996). For a typical image, this resulted in about 100 sources brighter than 5σ , out of which all but a few (see below) were subsequently identified by eye as false positives (e.g., image artifacts, cosmic-ray residuals, PSF distortion, and sources near the rim of the circular field of view which were in the input but not in the reference frame). The PSFs of the resulting candidates were then verified against those of stars in the input images.

The efficiency, ϵ , of recovering transients in the difference images was modeled with Monte Carlo simulations. Here a subset of the survey data was enriched with PSF-matched artificial point sources and subsequently passed through the image subtraction pipeline. The efficiency was then calculated from the ratio of recovered to input test sources. In total we obtained 1.9 million efficiency points with random location in the field and random magnitudes of $14 < B < 23$. As the main driver for our survey was the search for events in nearby galaxies, understanding ϵ as function of the local surface brightness became important. Thus, a subset of the efficiency points was placed inside the extend of the bright Fornax Cluster members. As expected, ϵ was found to decrease with increasing background flux contribution (see Fig. 4a). For “empty” locations ($B \sim 22.6 \text{ mag arcsec}^{-2}$) a recovery efficiency of $\epsilon = 0.85$ (0.7) was achieved for sources brighter than $B = 20$ (21.3). In positions with higher surface brightness ($B \sim 21.5, 20.0 \text{ mag arcsec}^{-2}$) the maximum efficiency was lower ($\epsilon = 0.60, 0.40$). Figure 4b shows ϵ as function of surface brightness for three test source magnitudes.

In a second step we performed a catalog-based variability search. While this method is inferior to image subtraction for sources overlaying the bright cluster galaxies, it improves the

⁶ IRAF is distributed by the National Optical Astronomy Observatory, which is operated by the Association of Universities for Research in Astronomy (AURA), Inc., under cooperative agreement with the National Science Foundation.

⁷ VizieR Online Data Catalog, 1297 (N. Zacharias et al. 2005).

⁸ See <http://www.astro.caltech.edu/~pick/ASCFIT/README.ascfit3.html>.

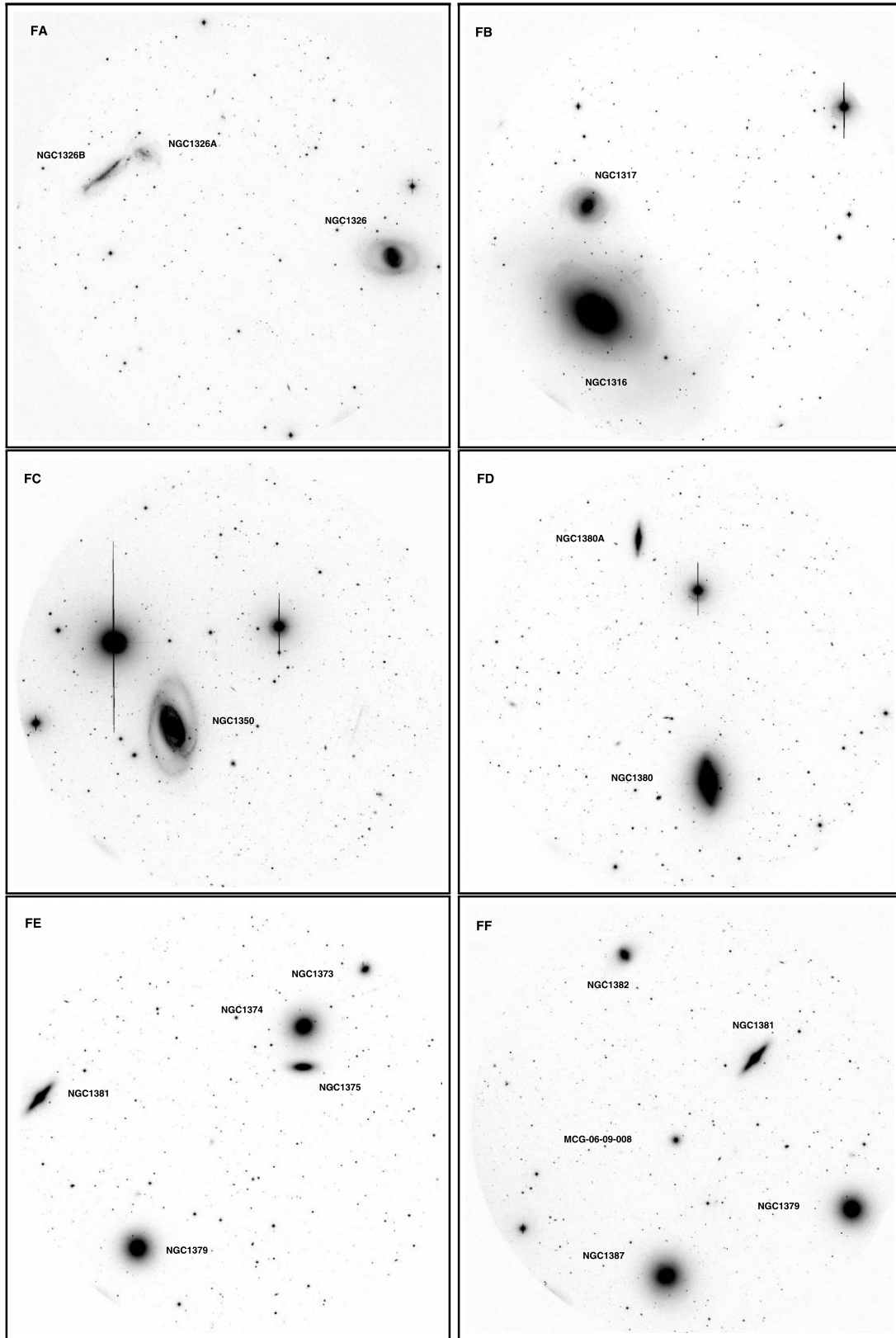


FIG. 1.—Survey fields. Prominent galaxies are marked. North is up and east to the left. Images are 25' on each side.

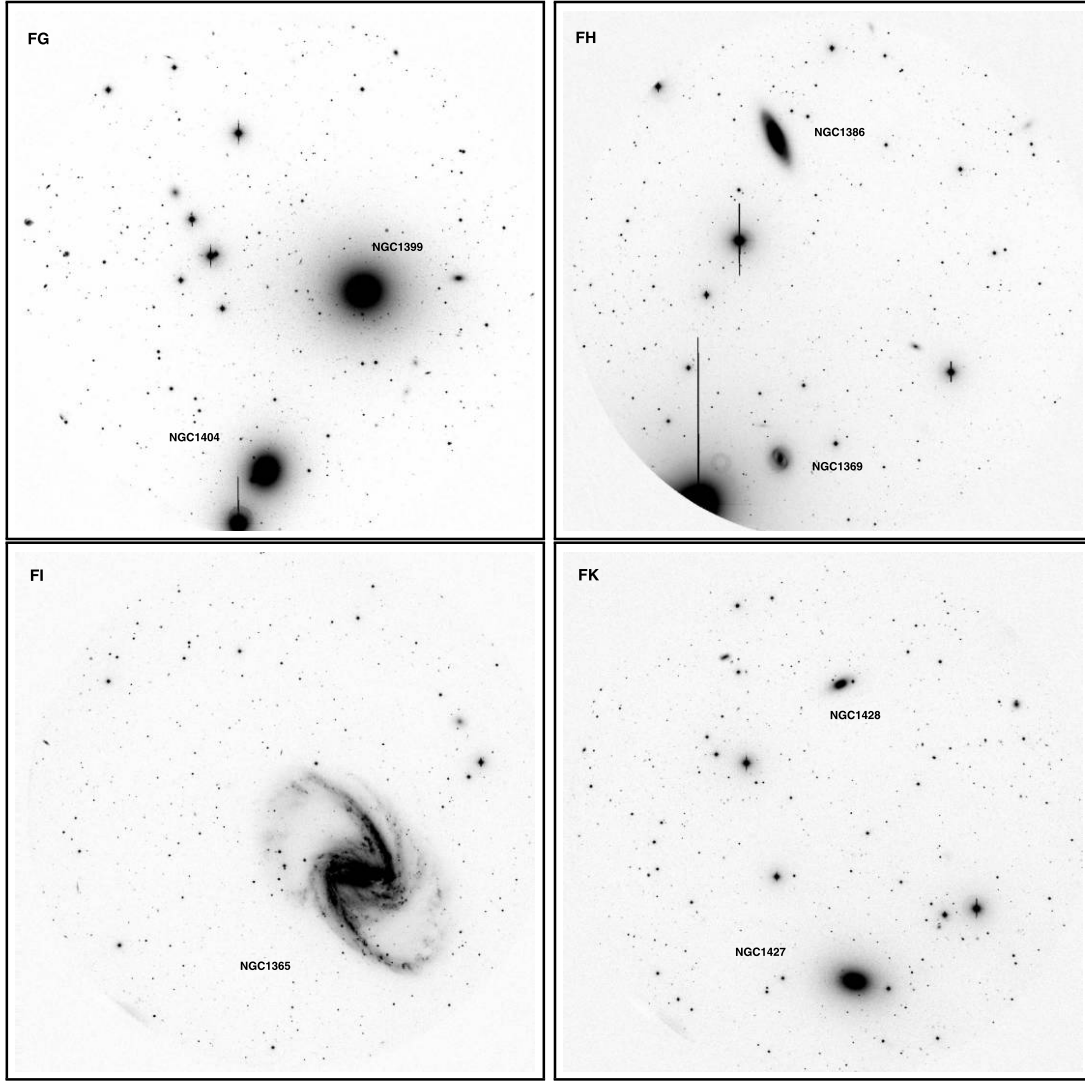


FIG. 1—*Continued*

TABLE 2
OBSERVATION LOG

Date (UT)	Exposures ^a									
	A	B	C	D	E	F	G	H	I	K
2006 Oct 23	10	10	10	10	10	9	8	8	8	10
2006 Oct 24	13	14	13	12	14	10	13	13	13	13
2006 Oct 25	Lost due to bad weather.									
2006 Nov 17	1	1	1	1	1	1	1	1	1	1
2006 Nov 18	1	1	1	1	1	1	1	1	1	1
2006 Nov 19	1	1	1	1	1	1	1	1	1	1
2006 Nov 20	1	1	1	1	1	1	1	1	1	1
2006 Nov 21	1	1	1	1	1	1	1	1	1	1
2006 Dec 19	14	15	14	14	14	14	14	14	14	14
2006 Dec 20	13	13	13	14	13	14	14	14	14	14
2006 Dec 21	12	12	12	12	12	12	12	10	12	12
Total ^b	67	69	67	67	68	64	66	64	66	68

^a Number of 120 s *B*-band exposure for each field in a given night.

^b Total number of observations for each field.

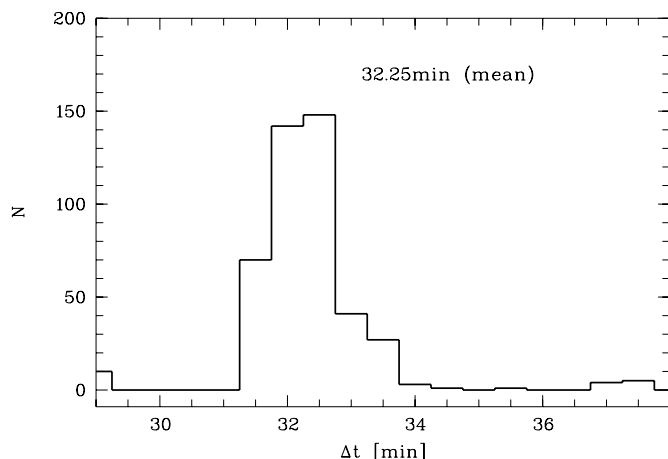


FIG. 2.—Time between two consecutive images of a given pointing. The mean cadence is 32.25 minutes.

detectivity of low-amplitude, bright variables in the field. For these, image subtraction is typically very sensitive to PSF stability, convolution, and alignment, and residuals unrelated to intrinsic variability may remain. The source catalogs were compiled using SExtractor, version 2.5.0 on the photometrically calibrated images (see above). Objects with two or more detections brighter than $B = 20$ and deviations of more than $B = 0.1$ mag from their median brightness were selected as candidate variables.

A serious contamination in optical transient and variable searches can come from solar system bodies. However, due to the high ecliptic latitude ($\beta \approx -53^\circ$) observations of the Fornax Cluster are only marginally affected. Our choice of using the B -band filter further reduced the impact of asteroids, whose emission peaks at longer wavelength. Moreover, repetitive visits of each field throughout the nights were allowing secure astrometric identification of moving objects with proper motions as low as $3'' \text{ day}^{-1}$. For example, the expected parallax of a Kuiper Belt object, at 100 AU from the Sun at that location and time of the year, is $\sim 33''$ and $\sim 3.5'' \text{ day}^{-1}$ due to the Earth and object motion, respectively. Thus, it was not surprising that only one astrometrically variable object was found in the survey data set.

3. RESULTS

The search netted seven high-confidence photometric transients and variables. Two, both of them earlier reported Type Ia SNe in NGC 1316, SN 2006dd (Monard 2006) and SN 2006mr (Monard & Folatelli 2006), were only detected in image subtraction. The remaining five objects were variable point sources found with both detection methods. None of them was previously cataloged in SIMBAD,⁹ NED,¹⁰ GCVS,¹¹ or detected in the *ROSAT* PSPC all-sky survey (Voges et al. 1999). Below we provide a brief description for each of these variable sources (see also Table 3).

3.1. Eruptive Variables

Two of the variable sources were detected when they exhibited single flares from their otherwise constant quiescent brightness. The first, FA-1 (Fig. 5a), is a faint, $B = 19.17 \pm 0.03$, point source that showed a distinct outburst with $\Delta B = 0.26 \pm 0.04$ mag (Fig. 6a; see also Table 4). The rise time to peak was shorter than 1 hr ($2 \times$ cadence) and the decline lasted over ~ 2.5 hr.

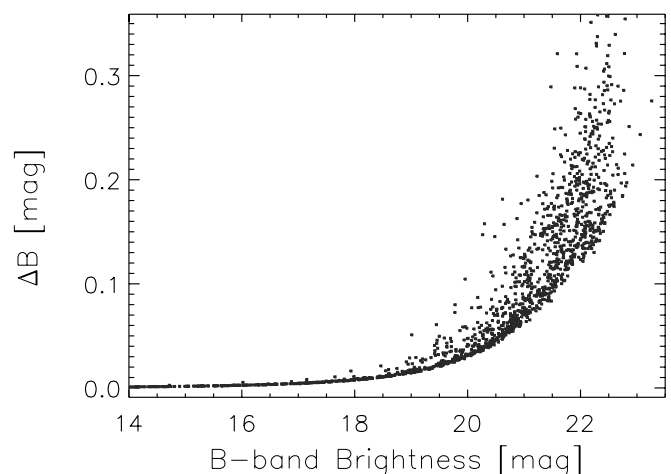


FIG. 3.—Photometric accuracy. Shown are the combined point source measurements of three exposures obtained on 2006 December 19 UT. The seeing was $1.4''$ and a 5σ limiting magnitude of $B \sim 22$ mag was reached. Sources brighter than $B \sim 15$ mag are saturated.

The source has a bright near-IR counterpart as detected by 2MASS¹² ($J = 14.58 \pm 0.03$, $K = 13.65 \pm 0.04$). We fitted its $B - J = 4.59 \pm 0.04$ and $B - K = 5.52 \pm 0.05$ mag colors¹³ with stellar templates (Pickles 1998) and found them to be consistent with an M1–2 star. The most likely explanation is a low-amplitude long-decay flare of a UV Ceti-type Galactic M1–2 dwarf ($M_B \sim 11.5$ mag) at a distance of ~ 350 pc.

FH-1 (Fig. 5d) was detected when it underwent a strong flare, with $\Delta B = 2.06 \pm 0.15$ mag. It rose to peak in less than 1 hr and decayed to its quiescent brightness of $B = 20.70 \pm 0.09$ over 1.5 hr (Fig. 6d). FH-1 is bright in the near-IR ($J = 15.02 \pm 0.02$, $K = 14.29 \pm 0.07$), and its colors ($B - J = 5.68 \pm 0.10$, $B - K = 6.41 \pm 0.10$ mag) indicate an M3–4 stellar classification. We suggest that this outburst was a long-decay flare of an M3–4 dwarf ($M_B \sim 12.5$ mag) at a distance of ~ 450 pc.

3.2. Periodic Variables

Regular brightness modulations were shown by three sources. FE-1 (Fig. 5c) displayed a nearly sinusoidal variability (Fig. 6c) with a maximum amplitude of $\Delta B = 0.31 \pm 0.05$ mag. A Lomb-Scargle periodogram (Scargle 1982) of the heliocentric corrected light curve revealed two possible periods, one at 0.19025 ± 0.00002 days and another at twice this value (0.38050 ± 0.00004 days; Fig. 7). The latter is favored by an apparent difference of $\Delta B = 0.07 \pm 0.02$ mag in depth of two consecutive minima. Note that FE-1 was included in the overlap of two of our pointings (FE and FF) and thus has twice the data coverage (132 images) compared to the remaining candidates. 2MASS detected the source at $J = 15.53 \pm 0.05$ and $K = 15.16 \pm 0.15$, which, together with a mean brightness of $B = 16.18 \pm 0.09$, results in $B - J = 0.65 \pm 0.10$ and $B - K = 1.02 \pm 0.17$ mag. These colors suggest a spectral type of A7–F0. The source is also included in the *GALEX* (Martin et al. 2003) source catalog¹⁴ and independent photometry on archival images provides magnitudes FUV = 23.4 ± 0.1 and NUV = 19.04 ± 0.02 .

¹² See <http://www.ipac.caltech.edu/2mass>.

¹³ Here we assume that the 2MASS observations are representative of the quiescence (or median in case of the noneruptive sources discussed in § 3.2) brightness. This is supported by generally lower amplitudes in the near-IR compared to the B band.

¹⁴ At <http://galex.stsci.edu/GR2/?page=mastform>.

⁹ See <http://simbad.u-strasbg.fr>.

¹⁰ See <http://nedwww.ipac.caltech.edu>.

¹¹ See <http://heasarc.gsfc.nasa.gov/W3Browse/all/gcvsnvars.html>.

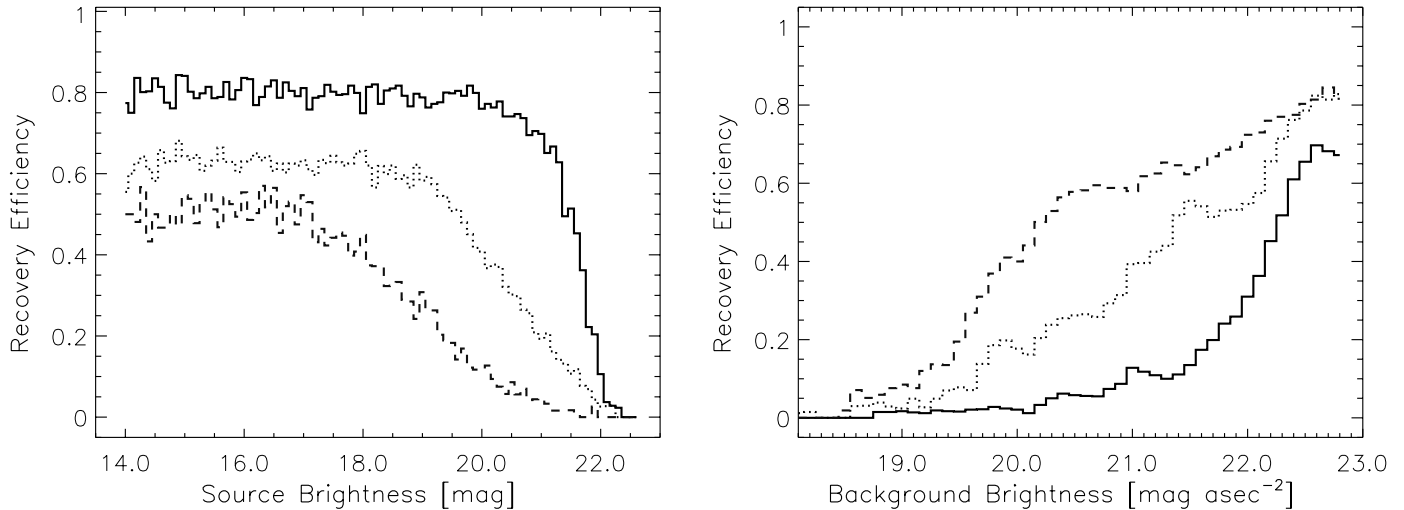


FIG. 4.—*Left*: Transient recovery efficiency as function of source magnitude for three levels of background surface brightness. The solid line ($B = 22.4 \text{ mag arcsec}^{-2}$) corresponds to the efficiency away from the Fornax Cluster members, while the dotted ($B = 21.5 \text{ mag arcsec}^{-2}$) and dashed ($B = 20.0 \text{ mag arcsec}^{-2}$) lines are representative for locations within the galaxies. Sources brighter than $B = 15$ are generally saturated. The faint sources cutoff corresponds to the 5σ detection limits in the difference images. *Right*: Transient recovery efficiency as function of background surface brightness for test sources with $B = 21.3$ (solid line), 19.5 (dotted line), and 18.0 (dashed line). Fewer efficiency points have been obtained at high surface brightness regions; thus, these bins have the lowest statistic.

A likely explanation for FE-1 is an eclipsing contact binary system of W UMa type with an orbital period of 0.38050 ± 0.00004 days. This is supported by the apparent two minima in the light curve which could indicate the phase of primary and secondary occultation.

The second periodic variable, FK-1 (Fig. 5e), was observed as a point source with mean brightness of $B = 15.42$ and regular nonsinusoidal variations with a period of 0.31864 ± 0.00006 days (Figs. 6e and 8). The maximum photometric amplitude was $\Delta B = 0.65 \pm 0.07$ mag. The source has a bright 2MASS counterpart ($J = 13.42 \pm 0.03$, $K = 12.93 \pm 0.03$), and its colors ($B - J = 2.00 \pm 0.20$, $B - K = 2.49 \pm 0.20$ mag) resemble those of a G0 9 giant or dwarf.

While the short modulation and light curve shape in principle resemble also that of an RRc Lyrae pulsator, the spectral type of G5–9 is inconsistent with this classification. The most likely interpretation for FK-1 is, similar to FE-1, a W UMa-type eclipsing binary.

The classification of the remaining variable, FB-1, is more challenging. Its light curve displayed apparently erratic variability

with an rms of 0.14 mag around the mean brightness of $B = 18.84 \pm 0.14$ and with a maximum amplitude of $\Delta B = 0.57 \pm 0.08$ mag (Fig. 6b). A Lomb-Scargle periodogram (Fig. 9) revealed a number of peaks, the most prominent being at a period of 0.0585 ± 0.0001 days (84.24 ± 0.15 minutes). However, the folded light curve shows several data points that deviate notably from this phasing. We also note that the power spectrum shows evidence for an additional period of ~ 107 minutes. Thus, the tentative timescale of modulation has to be taken with caution and confirmation by observations with higher sampling rate will be required.

FB-1 has no 2MASS counterpart to a limiting magnitude of $J = 17$, which constrains its color to $B - J < 1.84$ mag. This, together with a *GALEX* detection at $\text{NUV} = 21.39^{+0.56}_{-0.37}$ and a nondetection in the FUV filter to >21 mag, restricts a stellar classification to A–G. A spectrum obtained with the ESO Multi-Mode Instrument (EMMI) at the New Technology Telescope (NTT) in La Silla shows a blue continuum with prominent Balmer absorption lines (Fig. 10). A comparison with template stellar spectra (Pickles 1998) suggests an A7 classification. This

TABLE 3
SUMMARY OF DETECTED SOURCES

Source	R.A. _{J2000.0}	Decl. _{J2000.0}	B_{peak}^a (mag)	$B_{\text{quiescence}}^b$ (mag)	Classification	D_{proj}^c
FA-1	03 24 24.56	−36 30 26.5	18.91 ± 0.03	19.17 ± 0.03	M1–2	36 kpc to NGC 1326
FB-1	03 22 31.38	−37 04 01.5	18.48 ± 0.02	18.84 ± 0.14	(?) δ Scuti/SX Phe	26 kpc to NGC 1317
FE-1	03 36 18.85	−35 14 58.9	16.07 ± 0.01	16.18 ± 0.09	W UMa	29 kpc to NGC 1381
FH-1	03 36 53.67	−36 05 29.9	18.66 ± 0.03	20.70 ± 0.09	M3–4	42 kpc to NGC 1386
FK-1	03 42 33.73	−35 18 29.0	15.20 ± 0.01	15.42 ± 0.20	W UMa	35 kpc to NGC 1427
SN 2006dd	03 22 41.64	−37 12 13.2	17.25 ± 0.03^d	...	SN Ia	1.2 kpc to NGC 1316
SN 2006mr	03 22 42.84	−37 12 28.5	16.16 ± 0.03^e	...	SN Ia	1.1 kpc to NGC 1316

NOTE.—Units of right ascension are hours, minutes, and seconds, and units of declination are degrees, arcminutes, and arcseconds.

^a Observed peak B -band magnitude.

^b Observed mean (for periodic variables) or quiescence (for eruptive variables) B -band magnitude.

^c Projected distance to center of nearest Fornax Cluster galaxy.

^d Observed B -band magnitude on 2006 October 23.13 UT.

^e Observed B -band magnitude on 2006 November 17.58 UT.

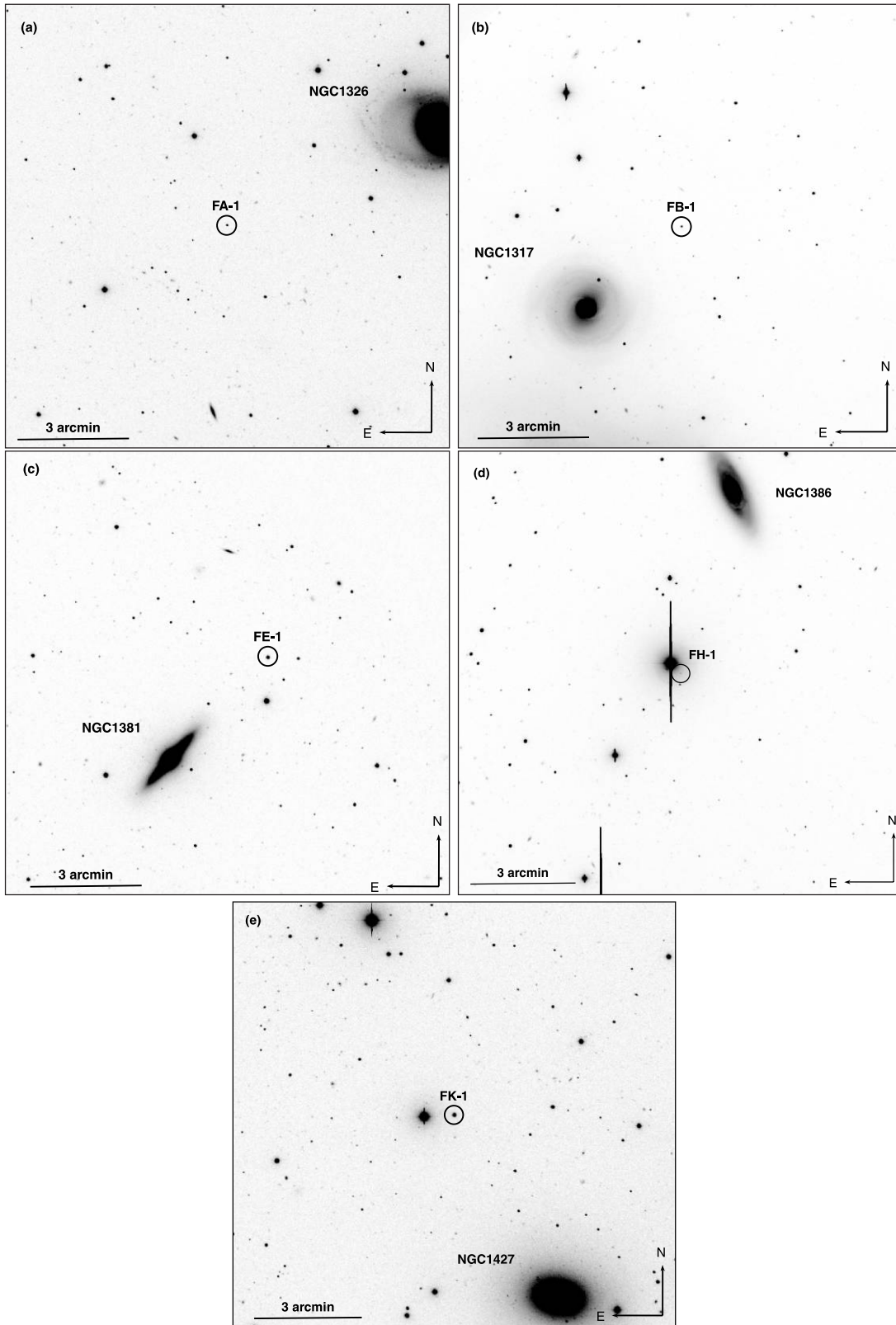


FIG. 5.—Finding charts.

spectral range is populated by pulsators such as δ Scuti stars and RR Lyrae. Of those, only δ Scuti stars, and the phenomenologically¹⁵ similar SX Phe stars (Rodríguez et al. 1990), exhibit

¹⁵ δ Scuti and SX Phe stars are generally distinguished by their hosting stellar population and metallicity. This cannot be accomplished with the available data.

modulations on timescales as short as those detected for FB-1. As indicated by the number of short period peaks in the periodogram, we may also have to consider events with periods below 84 minutes. Some white dwarf systems do show periodic pulsations below 30 minutes. ZZ Ceti-type sources have white dwarf temperatures (11–12 kK; Bergeron et al. 2004), in

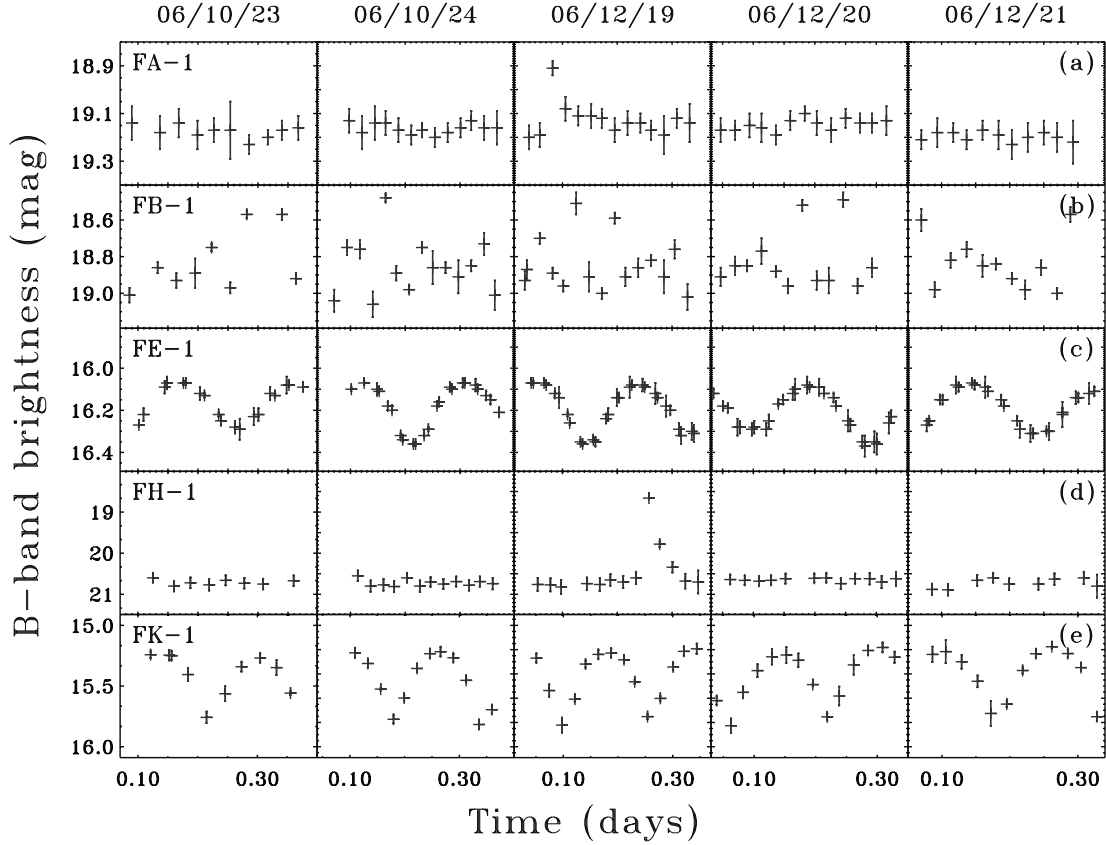


FIG. 6.—Observed B -band measurements for the five candidate variables listed in Table 3. Shown are the light curves for the five nights with multiple exposures per field (2006 October 23 and 24 and December 19, 20, and 21 UTC). Time is given in fractional days (UTC). See Table 4 for a compilation of data.

agreement with the observed colors (Kawka et al. 2006). However, the lack of pressure broadening of the Balmer absorption lines rules out the white dwarf scenario. Awaiting further test of the periodic modulation, we find that a Galactic δ Scuti or SX Phe star appears to be the most intriguing interpretation for FB-1.

4. DISCUSSION

Here we report the results of a dedicated search for optical fast transients and variables in the environment of the Fornax I galaxy cluster. In total, the survey netted two transients and five

high-amplitude ($\Delta B > 0.1$ mag) variable sources. Both transients have been detected as a result of the intermonth sampling of our observations and have independently been reported and classified as Type Ia supernovae in NGC 1216 (Monard 2006; Monard & Folatelli 2006). The properties of the five variables suggests that they are located in the foreground to the Fornax I Cluster and belong to the Milky Way stellar population. This is in agreement with the large projected distance (26–42 kpc) of the events to the nearest Fornax galaxies (see Table 3). Two of the variables were identified as flares from M dwarfs, while other two are likely eclipsing binaries of the W Uma type. The remaining variable shows indications for a very short periodicity (~ 84 minutes), and spectroscopy suggests it to be a δ Scuti or SX Phe star. No genuine fast transient brighter than $B = 21.3$ has been detected.

Surveys, like the one presented here, can offer valuable guidance for the planning and execution of the next generation of transient experiments. In order to provide relevant event rates, a complete identification of all sources detected with a given choice of cadence, filter, depth, amplitude, and field selection, is required. This will pose inevitable challenges for follow-up limited projects like Pan-STARRS and LSST. However, at least for variables, multiband photometry and good temporal coverage can already be strong indicators for the nature of an event, as demonstrated for the Fornax sources. Indeed, automatic cross-matching with UV to near-IR source catalogs with a similar depth as the surveys will be vital for the success of the future large optical projects.

4.1. All-Sky Rate of Fast Transients

In the following, we will discuss the estimates and expectations for transients on timescales of ~ 32 minutes and with apparent

TABLE 4
DATA TABLE FOR VARIABLE FOUND IN THE SURVEY

MJD	B -Band Mag	Error
FA-1		
54,031.09131.....	19.14	0.07
54,031.13743.....	19.18	0.07
54,031.16762.....	19.14	0.06
54,031.19747.....	19.19	0.06
54,031.22753.....	19.17	0.05
54,031.25564.....	19.17	0.12
54,031.28432.....	19.23	0.04
54,031.31550.....	19.20	0.03
54,031.34153.....	19.17	0.04
54,031.36836.....	19.16	0.05

NOTE.—Table 4 is published in its entirety in the electronic edition of the *Astrophysical Journal*. A portion is shown here for guidance regarding its form and content.

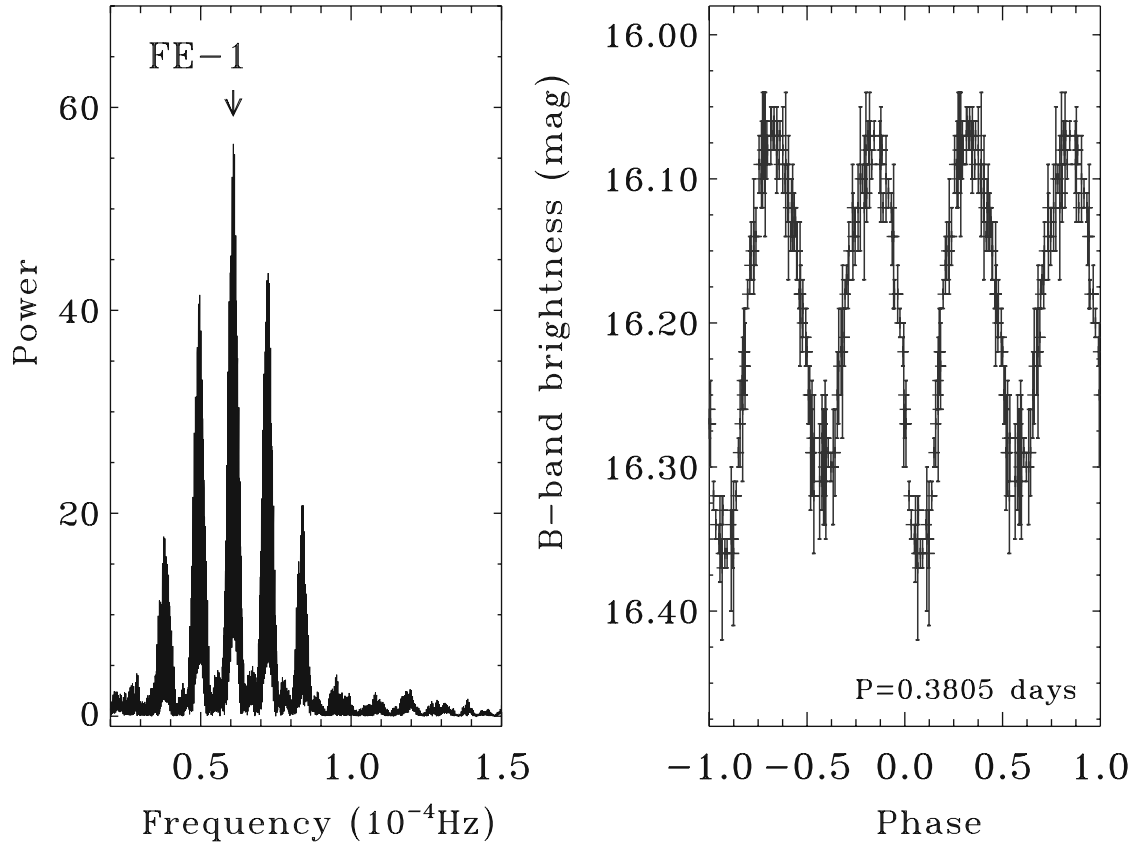


FIG. 7.—Lomb-Scargle periodogram (*left*) for FE-1 showing that the highest power occurs for at a frequency of $(6.083 \pm 0.001) \times 10^{-5}$ Hz (or period of 0.19025 ± 0.00002 days). The phase folded heliocentric corrected light curve (*right*) indicates differences in the depth of consecutive minima, suggesting that the real period is likely at twice the above value, 0.38050 ± 0.00004 days.

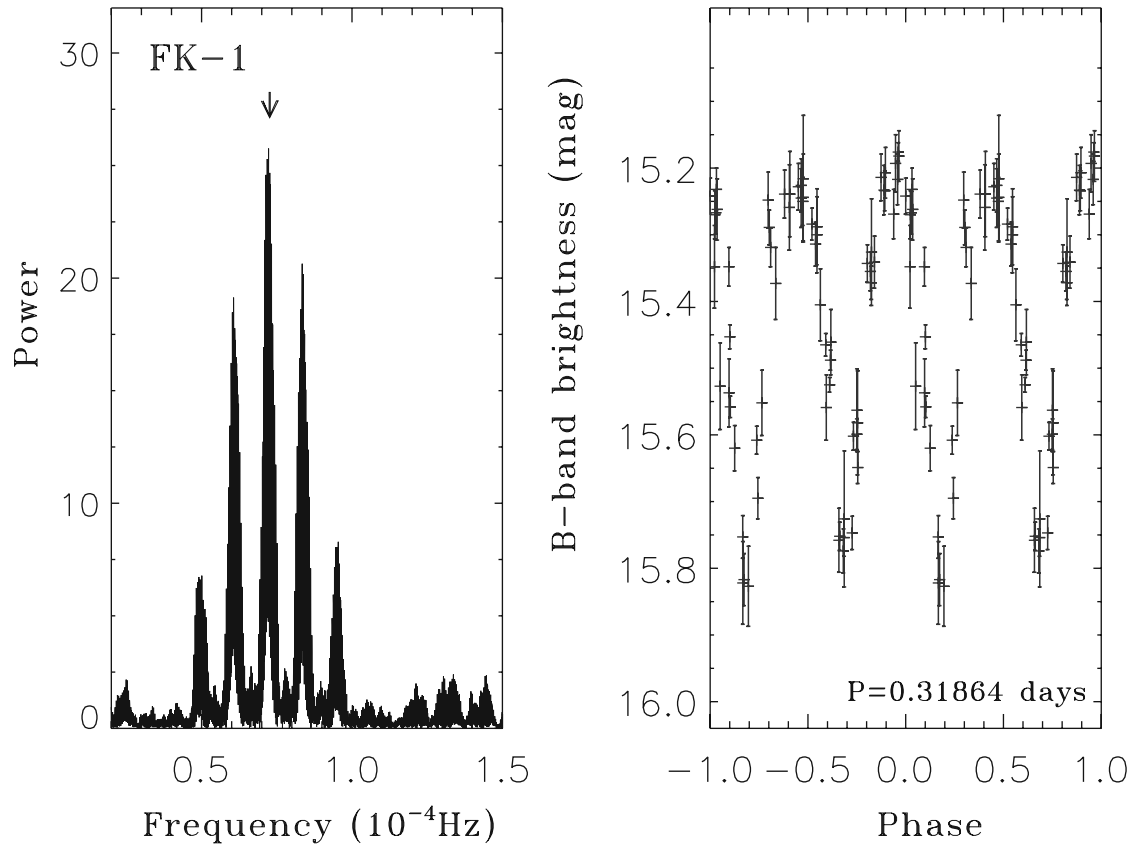


FIG. 8.—Same as Fig. 7, but for FK-1. The highest power occurs at a frequency of $(7.264 \pm 0.002) \times 10^{-5}$ Hz (or a period of 0.15932 ± 0.00003 days). The phase-folded heliocentric corrected light curve again indicates differences in the depth of consecutive minima, suggesting that the real period is likely 0.31864 ± 0.00006 days.

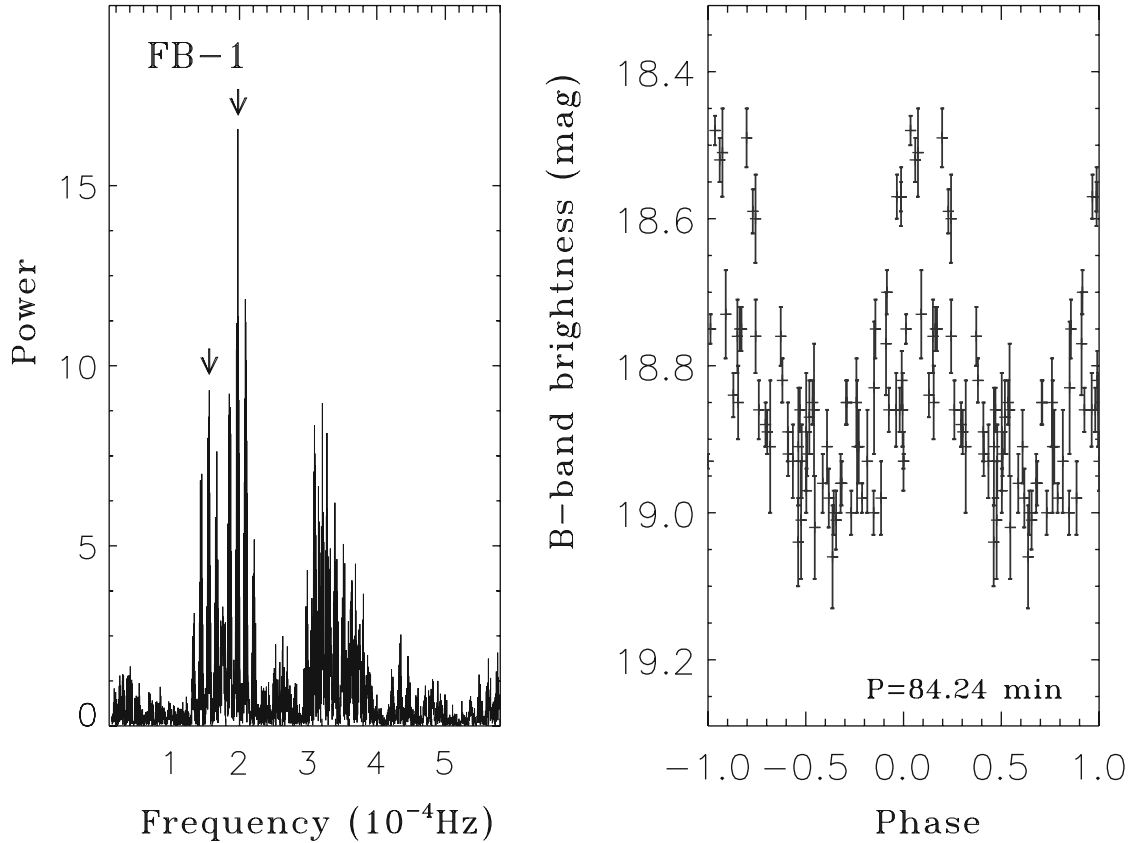


FIG. 9.— Same as Fig. 7, but for FB-1. The periodogram shows a large number of peaks, with the most prominent at $(1.975 \pm 0.005) \times 10^{-4}$ Hz (84.24 ± 0.15 minutes). A second period occurs at 107 minutes.

peak brightness of $15 < B < 21.3$. We start by determining the upper limit on the rate of cosmological fast transients not associated with any of the Fornax Cluster galaxies. As described in § 2, the areal survey exposure is $E_A = 1.86 \text{ deg}^2$ and the efficiency for a single detection of a field source brighter than $B = 21.3$ is $\epsilon = 0.7$. As we require a candidate to be found in at least two images, ϵ needs to be squared. The nondetection of fast transients

in the survey translates into a 95% Poisson upper limit of $N = 3$ events (Gehrels 1986). The corresponding rate follows from

$$r_A = \frac{N}{\epsilon^2 E_A}, \quad (1)$$

as $r_A < 3.3 \text{ events day}^{-1} \text{ deg}^{-2}$, or an annual all-sky rate of $r_A < 5 \times 10^7$. Note that these limits are valid only for an event population that is homogeneously distributed over the sky. In other words, the detection probability has to be independent of the field selection. Under this assumption, we can match our estimates with previously obtained results, e.g., from the Deep Lens Survey (DLS) transient search (Becker et al. 2004). Indeed, the Fornax survey is very similar to the DLS with respect to exposure (1.38 vs. 1.1 deg² days) and probed timescale (32 vs. 22 minutes). As also no genuine fast transient was found in the DLS, the event rate is comparable.

4.2. Rates of Fast Transients in Nearby Galaxies

The main motivation of our survey was the exploration of the transient and variable population in a specific environment, namely, in a galaxy cluster with known distance and known stellar mass. For this purpose, we now calculate the specific rate of fast transients per unit stellar mass, or its proxy, the B -band luminosity.

As discussed above (see also Fig. 4), ϵ is not only a function of the magnitude of a transient, M_T , but depends also on the underlying surface brightness, m_{SB} . Similarly, the product of the luminosity, $L_{SB,i}$, enclosed in a surface brightness bin, $m_{SB,i}$, and the relative exposure, t , is different for all targeted Fornax galaxies. Here, t denotes the time a given galaxy was probed for transients

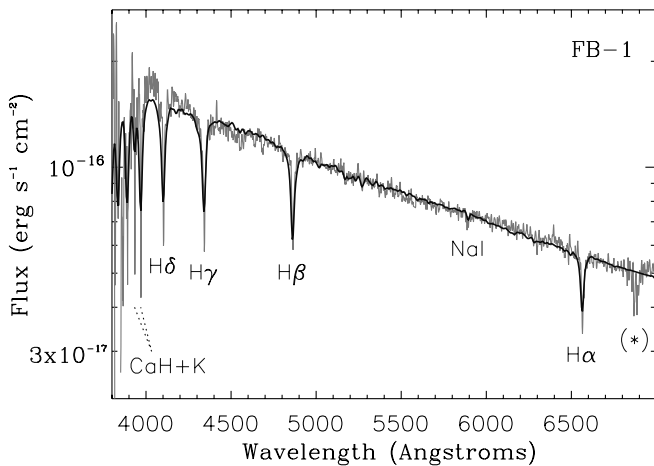


FIG. 10.— NTT EMMI spectrum (gray) of FB-1 obtained on 2007 December 12.19 UT using the low-dispersion mode (RILD) with grism 5 (instrumental FWHM = 4.5 Å). The data were reduced with customized IRAF routines and flux calibrated in comparison to the spectrophotometric standard star LTT377 (Hamuy et al. 1992). The black solid line shows an A7V template spectrum from Pickles (1998). Prominent spectral features are indicated.

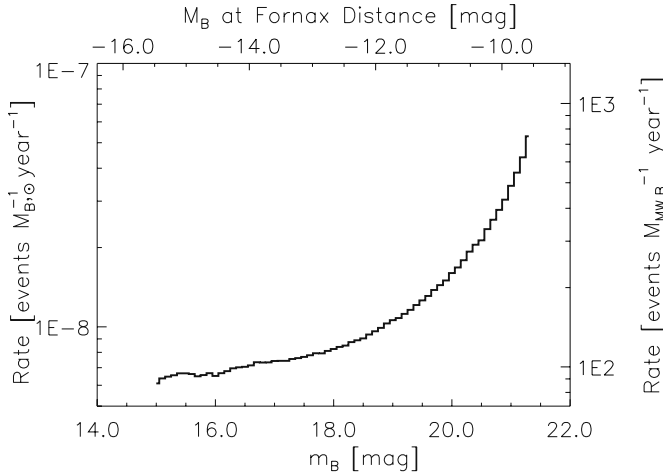


FIG. 11.— The 95% Poisson upper limit on the rate of transients on timescales of 32 minutes as function of peak brightness.

on timescales of the 32 minute cadence. We start by calculating $L_{SB,i}$ for each galaxy listed in Table 1, with i running from the saturation limit of 16.7 mag arcsec⁻² to the sky background brightness of 22.6 mag arcsec⁻² in steps of 0.1 mag. Next we estimate the survey exposure, $E_{SB,i}$, for each $m_{SB,i}$ in units¹⁶ of $M_{B,\odot}$ yr by summing $L_{SB,i}t$ for all galaxies. The rate of transients as function of the brightness can then be calculated as

$$r(M_T) = \sum_i \frac{N(M_T)}{\epsilon(M_T, m_{SB})_i^2 E_{SB,i}}. \quad (2)$$

Formerly, the number of detected transients, N , also depended on the peak brightness. However, here we use again the 95% Poisson upper limit of $N(M_T) = N = 3$ events, as no event in the entire probed range of $15 < B < 21.3$ was detected.

The result is presented in Figure 11, where we show the upper limit on the rate as function of transient magnitude. As expected, the brightest events ($m_B < 18.5$, $M_B < -12.4$) have the lowest limits ($r < 10^{-8}$ events $M_{B,\odot}^{-1}$ yr⁻¹). For the Milky Way disk ($M_B = -19.9$; Quillen & Sarajedini 1998) this translates into < 140 events yr⁻¹, e.g., a few times more than the classical novae rate. One could argue that any Galactic transient population brighter than classical novae and with a comparable frequency may have been discovered already. However, the short timescales tested in our survey require a significantly higher cadence than typically used in transient searches. Fast transients may have previously been detected in single images, but simply discarded as unconfirmed or spurious events. However, there have been a number of planetary transit and variable-star studies that offer

the required high cadence (e.g., Kane et al. 2005; Kraus et al. 2007; Lister et al. 2007). These experiments typically target dense Galactic fields and thus a large stellar population. Unfortunately, results on transients, as opposed to transits, are rarely recorded or published.

5. CONCLUSION

The existence of fast transients requires further constraint with specialized experiments. The most exciting facility in this respect will be the Palomar Transient Factory (PTF; A. Rau et al. 2008, in preparation), a dedicated transient survey instrument at the Palomar 48 inch (1.2 m) telescope with expected first light in winter 2008. The PTF will use a 7.8 deg² field of view to perform a number of transient searches on various timescales. The large field of view will allow us to cover galaxy clusters with fewer pointings, thus increasing the total stellar mass observed at a given cadence.

However, we have shown that the probability of detecting a transient strongly depends on the local surface brightness. While this is not a surprising result, its relevance for future searches in nearby galaxies needs to be understood. There will always be the need for a compromise between limiting magnitude of an event to be detected and galaxy fraction covered. Larger apertures or longer exposures are not necessarily improving the detection probability for faint events. Although more source photons will be collected, also more host light is received and a larger extend of the galaxy will be above saturation. The main factor for success will be the image quality. At a given surface brightness, a narrower PSF will increase the signal-to-noise ratio and thus the probability for a detection.

We are grateful to Paul Price for providing his image subtraction code and to Carrol Wainwright for his contribution to the pipeline. We thank Mara Salvato, Mansi M. Kasliwal, and S. Bradley Cenko for discussion and constructive criticism. We thank the referee for his stimulating comments and suggestions. This work is based on in part on observations collected at the European Southern Observatory, Chile. This publication makes use of data products from the Two Micron All Sky Survey, which is a joint project of the University of Massachusetts and the Infrared Processing and Analysis Center, California Institute of Technology, funded by the National Aeronautics and Space Administration (NASA) and the National Science Foundation (NSF). This research has made use of the NASA/IPAC Extragalactic Database (NED), which is operated by the Jet Propulsion Laboratory, California Institute of Technology, under contract with the NASA. This work is supported in part by grants from the NSF and NASA.

Facilities: Du Pont, NTT

¹⁶ Here we use an absolute solar B -band magnitude of $M_{B,\odot} = 5.48$.

REFERENCES

- Alard, C. 2000, A&AS, 144, 363
 Becker, A. C., et al. 2004, ApJ, 611, 418
 Bergeron, P., et al. 2004, ApJ, 600, 404
 Bertin, E., & Arnouts, S. 1996, A&AS, 117, 393
 Gehrels, N. 1986, ApJ, 303, 336
 Grillmair, C. J., et al. 1999, AJ, 117, 167
 Hamuy, M., et al. 1992, PASP, 104, 533
 Kaiser, N., et al. 2002, in Proc. SPIE, 4836, 154
 Kane, S. R., et al. 2005, MNRAS, 362, 117
 Kasliwal, M. M., et al. 2008, ApJ, 678, 1127
 Kawka, A., et al. 2006, ApJ, 643, L123
 Klotz, A., Boer, M., & Atteia, J. 2007, GCN Circ. 6769, <http://gcn.gsfc.nasa.gov/gcn3/6769.gcn3>
 Kraus, A. L., et al. 2007, AJ, 134, 1488
 Kulkarni, S. R., & Rau, A. 2006, ApJ, 644, L63
 Kulkarni, S. R., et al. 2007, Nature, 447, 458
 Landolt, A. U. 1992, AJ, 104, 340
 Lister, T. A., et al. 2007, MNRAS, 379, 647
 Martin, C., et al. 2003, in Proc. SPIE, 4854, 336
 Monard, L. A. G. 2006, CBET, 553
 Monard, L. A. G., & Folatelli, G. 2006, CBET, 723
 Morales-Rueda, L., et al. 2006, MNRAS, 371, 1681

- Ofek, E. O., et al. 2007, *ApJ*, 659, L13
———. 2008, *ApJ*, 674, 447
Pagani, C., et al. 2007, GCN, 6489, <http://gc.gsfc.nasa.gov/gcn3/6489.gcn3>
Pastorello, A., et al. 2007, *Nature*, 447, 829
Pickles, A. J. 1998, *PASP*, 110, 863
Quillen, A. C., & Sarajedini, V. L. 1998, *AJ*, 115, 1412
Quimby, R. M., et al. 2007, *ApJ*, 668, L99
Ramsay, G., et al. 2006, *MNRAS*, 371, 957
Rau, A., et al. 2007, *ApJ*, 659, 1536
Rodriguez, E., Rolland, A., & Lopez de Coca, P. 1990, *Ap&SS*, 169, 113
Rykoff, E. S., et al. 2005, *ApJ*, 631, 1032
Scargle, J. D. 1982, *ApJ*, 263, 835
Schlegel, D. J., Finkbeiner, D. P., & Davis, M. 1998, *ApJ*, 500, 525
Schmidt, B. P., et al. 2005, *BAAS*, 37, 457
Smith, N., et al. 2007, *ApJ*, 666, 1116
Stefanescu, A., et al. 2007, GCN, 6508, <http://gc.gsfc.nasa.gov/gcn3/6508.gcn3>
Tyson, A. 2005, in *ASP Conf. Ser.*, 339, *Observing Dark Energy*, ed. S. C. Wolff & T. R. Lauer (San Francisco: ASP), 95
van Dokkum, P. G. 2001, *PASP*, 113, 1420
Voges, W., et al. 1999, *A&A*, 349, 389